

Model Compounds for the Oxidized Uteroferrin–Phosphate Complex with Novel Dinucleating Ligands Containing Phenolate and Pyridine Donors

B. Krebs,^{*,†} K. Schepers,[†] B. Bremer,[†] G. Henkel,[†] E. Althaus,[‡] W. Müller-Warmuth,[‡]
K. Griesar,[§] and W. Haase[§]

Anorganisch-Chemisches Institut der Universität Münster, Wilhelm-Klemm-Strasse 8,
D-48149 Münster, Germany, Institut für Physikalische Chemie der Universität Münster,
Schlossplatz 4, D-48149 Münster, Germany, and Institut für Physikalische Chemie,
Technische Hochschule Darmstadt, D-64287 Darmstadt, Germany

Received August 26, 1993*

Novel dinucleating ligands containing phenol and pyridine were prepared, and their complexing properties toward Fe(III) are studied in order to model the active sites of purple acid phosphatases. Syntheses and crystal structures as well as magnetic, spectroscopic, and electrochemical properties of dinuclear Fe(III) complexes derived from 1,3-bis[(2-hydroxybenzyl)(2-pyridylmethyl)amino]-2-propanol (H_3bhpp), 1, and 2,6-bis[((2-hydroxybenzyl)(2-pyridylmethyl)amino)methyl]-4-methylphenol (H_3bhpmp), 2, are reported. $[Fe_2bhpp(O_2P(OPh)_2)_2]BPh_4 \cdot CHCl_3 \cdot CH_3OH$, 3, and $[Fe_2bhpmp(O_2P(OPh)_2)_2]ClO_4 \cdot H_2O$, 4, were synthesized and characterized by X-ray structure analysis. Both 3 and 4 crystallize in the triclinic space group $P\bar{1}$ with the following unit cell parameters: 3, $a = 14.883(6)$ Å, $b = 15.495(7)$ Å, $c = 18.149(8)$ Å, $\alpha = 98.11(4)^\circ$, $\beta = 103.59(4)^\circ$, $\gamma = 111.76(3)^\circ$, $Z = 2$; 4, $a = 10.526(3)$ Å, $b = 16.131(7)$ Å, $c = 19.741(9)$ Å, $\alpha = 84.34(4)^\circ$, $\beta = 74.47(3)^\circ$, $\gamma = 75.98(3)^\circ$, $Z = 2$. Besides the electronic and Mössbauer spectra and cyclovoltammograms the magnetic susceptibilities of 3 and 4 are examined in the temperature range 4.2–290.0 K.

Introduction

Purple acid phosphatases (PAP) are iron-containing non-heme proteins which catalyze the hydrolysis of activated phosphoric esters.^{1–7} The active sites of uteroferrin² and of the phosphatase from bovine spleen^{4–7} contain dinuclear iron units with two accessible oxidation states: The catalytically inactive, purple Fe^{III}–Fe^{III} form of PAP is characterized by a typical absorption maximum ($\lambda_{max} = 550$ –570 nm)¹ which is associated with a tyrosinate-to-Fe(III) charge-transfer transition. Treatment of the oxidized form with mild reductants results in formation of a high-spin, antiferromagnetically coupled Fe^{II}–Fe^{II} unit ($J = -19.8(5)$ cm⁻¹)⁸ representing the catalytically active pink species with an absorption maximum at 505–515 nm.¹ In the oxidized form both Fe(III) ions are high spin and antiferromagnetically coupled via yet unidentified bridging ligands. Magnetic susceptibility studies using various techniques yielded differing J values of $-J \geq 40$ and ≥ 150 cm⁻¹.^{2,4} These large values might suggest a μ -oxo bridge, which has been proved to be present in hemerythrin⁹ and ribonucleotide reductase,¹⁰ but until now there has been a lack of evidence from other methods for a (μ -oxo)-

diiron(III) core in the oxidized form of PAP. So far it has been controversial whether the tightly bound phosphate group which was detected in the purple form of PAP is bridging or terminally coordinated;¹¹ new EXAFS studies favor the O,O'-bridging coordination mode.^{11b} For the synthesis of model complexes for PAP, a coordination of phosphate and phosphate esters to binuclear Fe^{III}–Fe^{III} and Fe^{II}–Fe^{III} cores is of extraordinary importance. In previous studies diiron(II,III) and diiron(III,–III) model compounds containing a bridging coordination of phosphate and phosphate esters have been synthesized and characterized.^{12–17} Recently, a dinuclear iron(III) complex with a terminally coordinated phosphato ligand has been obtained using the dinucleating ligand *N,N,N',N'*-tetrakis(2-benzimidazolylmethyl)-2-hydroxy-1,3-diaminopropane (Htbpo).¹⁸ Poly-podal ligands like Htbpo have been proven to be suitable for the synthesis of dinuclear metal complexes due to the fact that they hold the two metal centers in close proximity. Several of these poly-podal ligands contain a bridging alcoholate or phenolate

* Anorganisch-Chemisches Institut, Universität Münster.

† Institut für Physikalische Chemie, Universität Münster.

‡ Institut für Physikalische Chemie, TH Darmstadt.

• Abstract published in *Advance ACS Abstracts*, April 1, 1994.

- (1) Antanaitis, B. C.; Aisen, P. *Adv. Inorg. Biochem.* 1983, 5, 111–113.
- (2) Lauffer, R. B.; Antanaitis, B. C.; Que, L., Jr. *J. Biol. Chem.* 1983, 258, 14212–14218.
- (3) Sage, J. T.; Xia, Y.-M.; Debrunner, P. G.; Keough, D. T.; de Jersey, J.; Zerner, B. J. *Am. Chem. Soc.* 1989, 111, 7239–7247 and references cited therein.
- (4) Averill, B. A.; Davis, J. C.; Burman, S.; Zirino, T.; Sanders-Loehr, J.; Loehr, T. M.; Sage, J. T.; Debrunner, P. G. *J. Am. Chem. Soc.* 1987, 109, 3760–3767.
- (5) Dietrich, M.; Münstermann, D.; Suerbaum, H.; Witzel, H. *Eur. J. Biochem.* 1991, 199, 105–113.
- (6) Cichutek, K.; Witzel, H.; Parak, F. *Hyperfine Interact.* 1988, 42, 885–888.
- (7) Vincent, J. B.; Olivier-Lilley, G. L.; Averill, B. A. *Chem. Rev.* 1990, 90, 1447–1467.
- (8) Day, E. P.; David, S. S.; Peterson, J.; Dunham, W. R.; Bonvoisin, J. J.; Sands, R. H.; Que, L., Jr. *J. Biol. Chem.* 1988, 263, 15561–15567.
- (9) Stenkamp, R. E.; Sieker, L. C.; Jensen, L. H. *J. Am. Chem. Soc.* 1984, 106, 618–622.

- (10) (a) Sjöberg, B. M.; Gräslund, A. *Adv. Inorg. Biochem.* 1983, 5, 87–90.
(b) Nordlund, P.; Sjöberg, B. M.; Ecklund, H. *Nature (London)* 1990, 345, 593–598.
- (11) (a) Kauzlarich, S. M.; Teo, B. K.; Zirino, T.; Burman, S.; Davis, J. C.; Averill, B. A. *Inorg. Chem.* 1986, 25, 2781–2785. (b) True, A. E.; Scarrow, R. C.; Randall, C. R.; Holz, R. G.; Que, L., Jr. *J. Am. Chem. Soc.* 1993, 115, 4246–4255.
- (12) Schepers, K.; Bremer, B.; Krebs, B.; Henkel, G.; Althaus, E.; Mosel, B.; Müller-Warmuth, W. *Angew. Chem.* 1990, 102, 582–584; *Angew. Chem., Int. Ed. Engl.* 1990, 29, 531.
- (13) Drücke, S.; Wieghardt, K.; Nuber, B.; Weiss, J.; Fleischhauer, H. P.; Gehring, S.; Haase, W. *J. Am. Chem. Soc.* 1989, 111, 8622–8631.
- (14) Armstrong, W. H.; Lippard, S. J. *J. Am. Chem. Soc.* 1985, 107, 3730–3731.
- (15) Turowski, P. N.; Armstrong, W. H.; Roth, M. E.; Lippard, S. J. *J. Am. Chem. Soc.* 1990, 112, 681–690.
- (16) Yan, S.; Cox, D. D.; Pearce, L. L.; Juarez-Garcia, C.; Que, L., Jr.; Zhang, J. H.; O'Connor, C. J. *Inorg. Chem.* 1989, 28, 2507–2509.
- (17) Norman, R. E.; Yan, S.; Que, L., Jr.; Backes, G.; Ling, J.; Sanders-Loehr, J.; Zhang, J. H.; O'Connor, C. J. *J. Am. Chem. Soc.* 1990, 112, 1554–1562.
- (18) Bremer, B.; Schepers, K.; Fleischhauer, P.; Haase, W.; Henkel, G.; Krebs, B. *J. Chem. Soc., Chem. Commun.* 1991, 510–512.

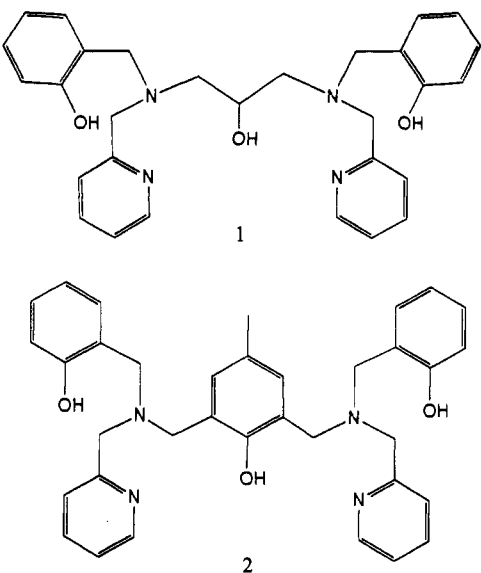


Figure 1. Ligands employed for the syntheses: 1,3-Bis[(2-hydroxybenzyl)(2-pyridylmethyl)amino]-2-propanol (H_3bhpp), 1, and 2,6-bis[((2-hydroxybenzyl)(2-pyridylmethyl)amino)methyl]-4-methylphenol (H_3bhpmp), 2.

Table 1. Crystallographic and Refinement Data for $[Fe_2bhpp(O_2P(OPh)_2)_2]BPh_4 \cdot CHCl_3 \cdot CH_3OH$, 3, and $[Fe_2bhpmp(O_2P(OPh)_2)_2]ClO_4 \cdot H_2O$, 4

	3	4
formula	$C_{79}H_{74}BCl_3Fe_2N_4O_{12}P_2$	$C_{59}H_{55}ClFe_2N_4O_{16}P_2$
M_r	1562.28	1285.20
cryst dimens, mm	$0.12 \times 0.15 \times 0.33$	$0.12 \times 0.15 \times 0.05$
radiation (λ , Å)	Mo K α (0.710 73)	Mo K α (0.710 73)
temp, K	150	170
space group	$P\bar{1}$	$P\bar{1}$
a , Å	14.883(6)	10.526(3)
b , Å	15.495(7)	16.131(7)
c , Å	18.149(8)	19.741(9)
α , deg	98.11(4)	84.34(4)
β , deg	103.59(3)	74.47(3)
γ , deg	111.76(3)	75.98(3)
V , Å 3	3655.6	3131.1
Z	2	2
D_{calc} , g/cm 3	1.418	1.362
μ , cm $^{-1}$	6.1	6.2
transm factor	0.78–0.89	0.88–0.94
index ranges	$-17 \leq h \leq 17$ $-18 \leq k \leq 18$ $0 \leq l \leq 20$	$-11 \leq h \leq 11$ $-18 \leq k \leq 18$ $0 \leq l \leq 22$
scan type	ω scan	$\omega-2\theta$ scan
2θ range, deg	4–48	4–48
no. of reflns measd	12 080	10 612
no. of reflns used	4994 ($I \geq 1.96\sigma(I)$)	4510 ($I > 1.96\sigma(I)$)
no. of variables used	930	760
R^a	0.079	0.097
R_w^b	0.069	0.094
GOF	1.05	1.39

^a $R = (\sum |F_o| - |F_c|)/\sum |F_o|$. ^b $R_w = [(\sum w(|F_o| - |F_c|)^2/\sum w F_o^2)]^{1/2}$; $w = 1/[\sigma^2 F_o + g F_c^2]$.

oxygen atom and pendant pyridine,^{19–23} pyrazole,^{24,25} imidazole,²⁶ and benzimidazole²⁷ groups as analogues of the histidine binding sites. We report here on the synthesis and characterization of the novel polypodal ligands 1,3-bis[(2-hydroxybenzyl)(2-pyri-

- (19) Karlin, K. D.; Hayes, J. C.; Gultneh, Y.; Cruse, R. W.; McKown, J. W.; Hutchinson, J. P.; Zubietta, J. *J. Am. Chem. Soc.* **1984**, *106*, 2121–2128.
- (20) Suzuki, M.; Kanatomi, H.; Murase, I. *Chem. Lett.* **1981**, 1745–1748.
- (21) Maloney, J. J.; Glogowski, M.; Rohrbach, D. F.; Urbach, F. L. *Inorg. Chim. Acta* **1987**, *127*, L33–L35.
- (22) Nishida, Y.; Shimo, H.; Maehara, H.; Kida, S. *J. Chem. Soc., Dalton Trans.* **1985**, 1945–1951.
- (23) Suzuki, M.; Sugisawa, T.; Senda, H.; Oshio, H.; Uehara, A. *Chem. Lett.* **1989**, 1091–1094.

ridylmethyl)amino]-2-propanol (H_3bhpp), 1, and 2,6-bis[((2-hydroxybenzyl)(2-pyridylmethyl)amino)methyl]-4-methylphenol (H_3bhpmp), 2.

Both ligands (Figure 1) represent, together with a similar phenoxo-bridging analogue reported very recently,²⁸ the first examples having mixed phenolate and pyridine pendant functionalities. Some properties of 1 and a preliminary report on an acetate-bridged analogue of 3 have been reported recently.²⁹ Furthermore, we will report the synthesis and properties of $[Fe_2bhpp(O_2P(OPh)_2)_2]BPh_4 \cdot CHCl_3 \cdot CH_3OH$, 3, and $[Fe_2bhpmp(O_2P(OPh)_2)_2]ClO_4 \cdot H_2O$, 4, which contain novel (μ -alkoxo)bis(μ -diphenyl phosphato)diiron(III) and (μ -phenoxo)bis(μ -diphenyl phosphato)diiron(III) cores as model compounds for active sites of PAP.³⁰

Experimental Section

2,6-Bis(chloromethyl)-4-methylphenol was synthesized by published procedures.³¹ For electrochemistry experiments, solvents and electrolytes were of electrochemistry grade or purified by distillation or recrystallization, respectively, prior to their use. All other reagents were purchased from commercial sources and used as supplied.

Preparation of Ligands and Complexes. **1,3-Bis[(2-hydroxybenzyl)(2-pyridylmethyl)amino]-2-propanol (H_3bhpp), 1.** 1,3-Diamino-2-propanol (4.5 g; 0.05 mol) and salicylaldehyde (12.2 g; 0.1 mol) were refluxed in ethanol (150 mL) for 30 min. The golden yellow solution was cooled to room temperature, and sodium borohydride (5 g; 0.132 mol) was added carefully in small portions. The solution was stirred overnight and refluxed for 1 h. The resulting solution was treated with 15 mL of concentrated hydrochloric acid, and when the gas evolution had ceased, a solution of sodium hydroxide (20 mL; 5 M) was added. Precipitated sodium borate was filtered off, and the volume of the filtrate was reduced by evaporation. The remaining crude bis(2-hydroxybenzyl)-1,3-diamino-2-propanol was extracted with chloroform and dried over sodium sulfate. The residue which was obtained after evaporation under reduced pressure was dissolved in absolute ethanol (50 mL), and the resulting mixture was treated with an aqueous solution of 2-pyridylmethyl chloride hydrochloride (19.67 g; 0.12 mol). During the following 5 days, a sodium hydroxide solution (8.8 g in 35 mL of water) was added in small portions so that the pH never exceeded 9. Precipitated sodium chloride was filtered off, and the solution was evaporated under reduced pressure. The remaining crude product was extracted with chloroform (50 mL) and dried over sodium sulfate. Evaporation of the organic layer yielded crude 1. For further purification the product was extracted with a mixture of 30 mL of methylene chloride and 200 mL of diethyl ether. Solid impurities were filtered off, and 6.75 g (28%) of a viscous yellow product was obtained. Mp: 128–129 °C. Anal. Calcd for $C_{29}H_{32}N_4O_3$: C, 71.90; H, 6.61; N, 11.57. Found: C, 71.25; H, 6.34; N, 11.18.

2,6-Bis[(2-hydroxybenzyl)(2-pyridylmethyl)amino)methyl]-4-methylphenol (H_3bhpmp), 2. (a) (2-Hydroxybenzyl)(2-pyridylmethyl)amine, 2-Picolylamine (10.8 g; 0.1 mol) and salicylaldehyde (12.2 g; 0.1 mol) was refluxed in ethanol (100 mL) for 30 min. The solution was cooled to room temperature, and sodium borohydride (5 g; 0.132 mol) was added

- (24) Sorell, T. N.; O'Connor, C. J.; Anderson, O. P.; Reibenspies, J. H. *J. Am. Chem. Soc.* **1985**, *107*, 4199–4206.
- (25) Sorell, T. N.; Jameson, D. L.; O'Connor, C. J. *Inorg. Chem.* **1984**, *23*, 190–195.
- (26) Oberhausen, K. J.; Richardson, J. F.; Buchanan, R. M.; McCusker, J. K.; Hendrickson, D. N.; Latour, J. M. *Inorg. Chem.* **1991**, *30*, 1357–1365.
- (27) (a) Berends, H. P.; Stephan, D. W. *Inorg. Chem.* **1987**, *26*, 749. (b) Berends, H. P.; Stephan, D. W. *Inorg. Chim. Acta* **1985**, *99*, L53–L55.
- (28) Campbell, V. D.; Parsons, E. J.; Pennington, W. T. *Inorg. Chem.* **1993**, *32*, 1773–1778.
- (29) Neves, A.; Erthal, S. M. D.; Drago, V.; Griesar, K.; Haase, W. *Inorg. Chim. Acta* **1992**, *197*, 121–124.
- (30) Abbreviations used: OBz, benzoate; OPr, propionate; OAc, acetate; bpmp, 2,6-bis[bis((2-pyridylmethyl)amino)methyl]-4-methylphenolate; Hpta, N,N' -bis[N,N'-bis(carboxymethyl)glycyl]-2-hydroxy-1,3-diaminopropane; Htbpo, Et-Htbpo, N,N,N',N' -tetrakis(2-benzimidazolylmethyl)-2-hydroxy-1,3-diaminopropane and its 1-ethylbenzimidazolyl derivative; Hxta, N,N' -(2-hydroxy-5-methyl-1,3-xyllyl)bis(N -carboxymethylglycine; L-bzim, 2,6-bis[bis((2-benzimidazolylmethyl)amino)methyl]-4-methylphenolate; hdp, N -(ω -hydroxybenzyl)- N,N -bis(2-pyridylmethyl)amine.
- (31) Borovik, A. S.; Papaefthymiou, V.; Taylor, L. F.; Anderson, O. P.; Que, L., Jr. *J. Am. Chem. Soc.* **1989**, *111*, 6183–6195.

Table 2. Atomic Coordinates and Isotropic Thermal Parameters (\AA^2) for Non-Hydrogen Atoms in 3

atom	<i>x</i>	<i>y</i>	<i>z</i>	<i>U</i> _{eq}	atom	<i>x</i>	<i>y</i>	<i>z</i>	<i>U</i> _{eq}
Fe(1)	0.02433(11)	0.17717(10)	0.22140(9)	0.0312(7)	C(29)	-0.1591(10)	0.0065(10)	0.2295(8)	0.073(7)
Fe(2)	0.24715(11)	0.39151(10)	0.32007(8)	0.0289(7)	C(30)	0.0076(8)	0.5256(8)	0.3010(6)	0.040(6)
Cl(1)	0.4245(8)	0.0891(5)	0.3081(5)	0.204(6)	C(31)	0.0726(9)	0.5838(8)	0.3739(7)	0.043(6)
Cl(2)	0.3499(9)	-0.0418(8)	0.3941(9)	0.297(9)	C(32)	0.1052(10)	0.6821(9)	0.3878(8)	0.058(7)
Cl(3)	0.5132(11)	-0.0298(7)	0.3372(11)	0.338(12)	C(33)	0.0709(11)	0.7224(10)	0.3311(8)	0.062(8)
P(1)	0.02058(23)	0.36458(21)	0.32814(17)	0.0373(14)	C(34)	0.0082(10)	0.6640(10)	0.2588(8)	0.067(8)
P(2)	0.16591(22)	0.20880(21)	0.38996(17)	0.0366(14)	C(35)	-0.0266(9)	0.5637(9)	0.2423(7)	0.049(6)
O(1)	0.1330(4)	0.2989(4)	0.2217(4)	0.024(3)	C(36)	-0.1142(8)	0.3394(9)	0.4039(6)	0.037(6)
O(2)	-0.0322(5)	0.2657(5)	0.2756(4)	0.042(4)	C(37)	-0.1467(10)	0.4082(10)	0.4262(7)	0.048(7)
O(3)	0.1337(5)	0.4111(5)	0.3552(4)	0.036(4)	C(38)	-0.2430(12)	0.3793(13)	0.4288(8)	0.069(9)
O(4)	-0.0250(5)	0.4261(5)	0.2803(4)	0.041(4)	C(39)	-0.3084(13)	0.2838(17)	0.4101(9)	0.084(11)
O(5)	-0.0104(5)	0.3711(5)	0.4051(4)	0.040(4)	C(40)	-0.2738(11)	0.2166(12)	0.3872(8)	0.070(8)
O(6)	0.2462(5)	0.2852(5)	0.3706(4)	0.032(3)	C(41)	-0.1763(10)	0.2409(9)	0.3826(7)	0.055(7)
O(7)	0.0693(5)	0.1516(5)	0.3252(4)	0.041(4)	C(42)	0.1725(9)	0.0707(9)	0.4564(7)	0.046(6)
O(8)	0.2190(5)	0.1452(5)	0.4224(4)	0.046(4)	C(43)	0.0855(11)	-0.0066(10)	0.4162(10)	0.077(8)
O(9)	0.1324(5)	0.2489(5)	0.4579(4)	0.046(4)	C(44)	0.0463(12)	-0.0787(11)	0.4521(11)	0.085(9)
O(10)	0.3498(5)	0.4919(5)	0.4007(4)	0.044(4)	C(45)	0.0938(12)	-0.0716(12)	0.5245(12)	0.095(10)
O(11)	0.0733(6)	0.0948(5)	0.1743(5)	0.050(4)	C(46)	0.1806(14)	0.0025(14)	0.5642(10)	0.110(11)
O(12)	-0.0326(20)	0.0896(18)	0.7799(16)	0.241(25)	C(47)	0.2227(11)	0.0780(11)	0.5315(8)	0.079(8)
N(1)	-0.0479(6)	0.1915(5)	0.1086(5)	0.029(4)	C(48)	0.1947(8)	0.3165(8)	0.5299(6)	0.039(6)
N(2)	-0.1291(7)	0.0750(6)	0.1924(6)	0.048(5)	C(49)	0.2986(9)	0.3604(9)	0.5505(7)	0.056(7)
N(3)	0.2580(7)	0.4893(5)	0.2436(5)	0.032(4)	C(50)	0.3539(10)	0.4266(9)	0.6215(8)	0.055(7)
N(4)	0.3527(6)	0.3685(6)	0.2643(5)	0.034(4)	C(51)	0.3055(11)	0.4498(9)	0.6703(8)	0.057(7)
B	0.6553(10)	0.3093(8)	0.9661(8)	0.036(6)	C(52)	0.2007(12)	0.4070(9)	0.6486(8)	0.060(8)
C(1)	0.1196(8)	0.3344(7)	0.1539(6)	0.029(5)	C(53)	0.1456(10)	0.3408(8)	0.5780(7)	0.048(6)
C(2)	0.1601(8)	0.4444(7)	0.1790(6)	0.034(5)	C(54)	0.5494(8)	0.3031(7)	0.9052(7)	0.036(6)
C(3)	0.0074(8)	0.2938(7)	0.1079(6)	0.031(5)	C(55)	0.4804(10)	0.3288(9)	0.9320(8)	0.053(7)
C(4)	0.2660(7)	0.5829(6)	0.2889(6)	0.026(5)	C(56)	0.3968(10)	0.3318(10)	0.8820(11)	0.070(9)
C(5)	0.3578(8)	0.6323(7)	0.3606(6)	0.037(5)	C(57)	0.3784(11)	0.3072(9)	0.8016(11)	0.067(8)
C(6)	0.4097(9)	0.7330(8)	0.3782(8)	0.050(7)	C(58)	0.4431(10)	0.2799(9)	0.7736(8)	0.056(6)
C(7)	0.4889(10)	0.7868(9)	0.4481(9)	0.062(7)	C(59)	0.5259(8)	0.2759(7)	0.8240(7)	0.038(5)
C(8)	0.5183(9)	0.7408(9)	0.4984(9)	0.058(7)	C(60)	0.7415(8)	0.4227(8)	0.9937(6)	0.032(6)
C(9)	0.4732(9)	0.6407(8)	0.4828(7)	0.046(6)	C(61)	0.7148(9)	0.5016(8)	0.9952(6)	0.039(6)
C(10)	0.3923(8)	0.5868(8)	0.4141(6)	0.038(6)	C(62)	0.7893(11)	0.5965(8)	1.0204(7)	0.050(7)
C(11)	0.3468(8)	0.5051(7)	0.2156(6)	0.038(6)	C(63)	0.8895(10)	0.6164(9)	1.0452(7)	0.047(7)
C(12)	0.3777(8)	0.4238(7)	0.2145(6)	0.033(5)	C(64)	0.9193(10)	0.5422(9)	1.0458(6)	0.048(6)
C(13)	0.4401(8)	0.4119(8)	0.1713(7)	0.041(6)	C(65)	0.8453(9)	0.4468(7)	1.0199(6)	0.040(6)
C(14)	0.4771(9)	0.3437(9)	0.1805(7)	0.047(6)	C(66)	0.6347(8)	0.2733(7)	1.0447(6)	0.035(6)
C(15)	0.4551(10)	0.2901(8)	0.2343(7)	0.049(7)	C(67)	0.7051(8)	0.3142(7)	1.1196(7)	0.039(6)
C(16)	0.3891(9)	0.3029(8)	0.2727(7)	0.042(6)	C(68)	0.6941(9)	0.2764(9)	1.1841(7)	0.044(7)
C(17)	-0.0464(8)	0.1215(7)	0.0428(6)	0.032(5)	C(69)	0.6080(10)	0.1932(10)	1.1749(8)	0.054(8)
C(18)	0.0567(8)	0.1261(7)	0.0487(7)	0.037(5)	C(70)	0.5375(9)	0.1533(9)	1.1017(7)	0.045(6)
C(19)	0.1114(10)	0.1106(7)	0.1158(8)	0.045(6)	C(71)	0.5478(8)	0.1912(7)	1.0384(6)	0.037(6)
C(20)	0.2092(10)	0.1125(8)	0.1200(9)	0.056(7)	C(72)	0.6983(8)	0.2403(7)	0.9200(6)	0.034(5)
C(21)	0.2468(11)	0.1310(9)	0.0587(11)	0.064(8)	C(73)	0.7660(8)	0.2749(8)	0.8782(6)	0.038(6)
C(22)	0.1954(11)	0.1463(8)	-0.0075(10)	0.059(8)	C(74)	0.8022(9)	0.2161(8)	0.8401(7)	0.048(6)
C(23)	0.0982(10)	0.1432(7)	-0.0124(7)	0.047(6)	C(75)	0.7724(9)	0.1215(9)	0.8429(7)	0.050(7)
C(24)	-0.1544(8)	0.1688(8)	0.1029(6)	0.044(6)	C(76)	0.7003(9)	0.0849(8)	0.8804(7)	0.047(6)
C(25)	-0.1979(8)	0.0854(7)	0.1361(6)	0.035(5)	C(77)	0.6656(8)	0.1426(7)	0.9180(6)	0.033(5)
C(26)	-0.3015(9)	0.0259(10)	0.1165(7)	0.058(7)	C(78)	0.4211(20)	0.0000(19)	0.3266(16)	0.157(18)
C(27)	-0.3320(10)	-0.0448(9)	0.1565(8)	0.067(7)	C(79)	0.0746(31)	0.1503(35)	0.7877(25)	0.266(36)
C(28)	-0.2595(12)	-0.0559(11)	0.2121(9)	0.094(9)					

carefully in small portions over a period of 2 h. The mixture was stirred overnight and refluxed for 1 h. To this solution concentrated was added hydrochloric acid. After a few minutes the solution was made alkaline with a sodium hydroxide solution (20 mL; 5 M). Sodium borate was filtered off, and the filtrate was evaporated under reduced pressure. The remaining crude product was extracted with chloroform and dried over sodium sulfate. (2-hydroxybenzyl)(2-pyridylmethyl)amine was obtained as a yellow oil after evaporation of the organic layer (18.35 g; 86%).

(b) **2,6-Bis((2-hydroxybenzyl)(2-pyridylmethyl)amino)methylphenol.** (2-hydroxybenzyl)(2-pyridylmethyl)amine (6.16 g; 28.8 mmol) and triethylamine (4.37 g; 43.2 mmol) were dissolved in 100 mL of methanol, and the solution was cooled to 0 °C. A solution of 2,6-bis(chloromethyl)-4-methylphenol (3 g; 14.6 mmol) in 20 mL of methanol was added dropwise. When the addition was complete, the resulting mixture was allowed to warm to room temperature and stirred overnight. The solution was concentrated under reduced pressure and extracted with 60 mL of chloroform. The organic layer was washed with water (3 × 30 mL) and dried over anhydrous sodium sulfate. 2 was obtained as a colorless powder after evaporation under reduced pressure, which was used without further purification (6.24 g; 76%). Mp: 87–90 °C. Anal. Calcd for C₂₅H₃₆N₄O₃: C, 75.00; H, 6.43; N, 11.43. Found: C, 74.27; H, 6.37; N, 11.07.

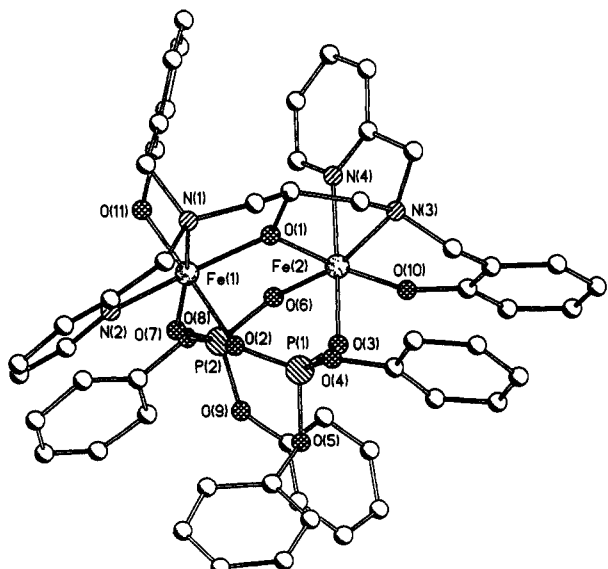
[Fe₂bhpp(O₂P(OPh)₂)₂]BPh₄·CHCl₃·CH₃OH, **3.** A solution of H₃bhpp (0.39 g; 0.8 mmol) in 15 mL of methanol was treated with a solution of Fe(ClO₄)₂·9H₂O (0.83 g; 1.6 mmol) in 15 mL of methanol. Addition of diphenyl phosphate (0.4 g; 1.6 mmol) in 20 mL of methanol and metathesis with sodium tetraphenylborate (0.83 g; 2.4 mmol) resulted in the immediate precipitation of crude **3**. Rod-shaped crystals of **3** were obtained by vapor diffusion of methanol into a chloroform/ethanol solution of **3**. [Fe₂bhpp(O₂P(OPh)₂)₂]BPh₄·CHCl₃·CH₃OH: yield 15%. Anal. Calcd for C₇₉H₇₄BCl₂Fe₂N₄O₁₂P₂: C, 60.74; H, 4.74; N, 3.59. Found: C, 60.35; H, 4.82; N, 3.52.

[Fe₂bhpmp(O₂P(OPh)₂)₂]ClO₄·H₂O, **4.** A solution of H₃bhpmp (0.45 g; 0.8 mmol) in 30 mL of methanol was treated with a solution of Fe(ClO₄)₂·9H₂O (0.83 g; 1.6 mmol) in 20 mL of methanol. Addition of diphenyl phosphate (0.2 g; 0.8 mmol) in 10 mL of methanol afforded compact platelike crystals. [Fe₂bhpmp(O₂P(OPh)₂)₂]ClO₄·H₂O: yield 23%. Anal. Calcd for C₅₉H₅₅ClFe₂N₄O₁₆P₂: C, 55.13; H, 4.28; N, 4.36. Found: C, 54.75; H, 4.33; N, 4.31.

Instrumentation and Physical Measurements. Melting points were obtained by using a Mettler melting point apparatus (FP 51) and are uncorrected. All elemental analyses were performed on a Hewlett Packard Scientific Model 185. Visible spectra of the complexes in CH₂Cl₂ were recorded with a Shimadzu UV 2100 spectrophotometer. Cyclic vol-

Table 3. Atomic Coordinates and Isotropic Thermal Parameters (\AA^2) for Non-Hydrogen Atoms in 4

atom	<i>x</i>	<i>y</i>	<i>z</i>	<i>U</i> _{eq}	atom	<i>x</i>	<i>y</i>	<i>z</i>	<i>U</i> _{eq}
Fe(1)	1.16672(20)	0.25316(12)	0.22400(11)	0.0352(9)	C(18)	1.3513(15)	0.0470(12)	0.3887(11)	0.063(9)
Fe(2)	0.84834(19)	0.18684(12)	0.21042(11)	0.0349(9)	C(19)	1.3595(14)	0.0201(10)	0.3239(9)	0.049(7)
P(1)	0.92570(36)	0.36857(23)	0.15581(20)	0.0355(15)	C(20)	1.3129(14)	0.0763(8)	0.2754(8)	0.047(7)
P(2)	1.15187(36)	0.13592(23)	0.10491(21)	0.0381(17)	C(21)	0.9494(14)	0.0413(8)	0.3069(7)	0.041(6)
Cl(1)	0.6955(8)	0.8470(3)	0.3996(3)	0.091(3)	C(22)	0.8451(14)	-0.0002(8)	0.2243(8)	0.043(6)
O(1)	0.9895(8)	0.2070(5)	0.2654(5)	0.036(4)	C(23)	0.7417(14)	0.0125(10)	0.1861(8)	0.043(7)
O(2)	1.0569(9)	0.3481(6)	0.1750(5)	0.044(4)	C(24)	0.6934(15)	-0.0568(10)	0.1740(8)	0.054(7)
O(3)	0.8455(9)	0.3030(6)	0.1669(5)	0.044(4)	C(25)	0.5989(17)	-0.0494(13)	0.1354(11)	0.073(10)
O(4)	0.8264(9)	0.4500(6)	0.1969(5)	0.048(5)	C(26)	0.5515(16)	0.0270(13)	0.1069(10)	0.067(9)
O(5)	0.9624(8)	0.3972(5)	0.0758(5)	0.038(4)	C(27)	0.5913(15)	0.1006(12)	0.1175(9)	0.065(8)
O(6)	1.2209(9)	0.1703(5)	0.1478(5)	0.044(4)	C(28)	0.6865(15)	0.0925(10)	0.1571(8)	0.047(7)
O(7)	1.0127(9)	0.1257(6)	0.1362(5)	0.045(4)	C(29)	0.7012(13)	0.0852(9)	0.3227(8)	0.051(7)
O(8)	1.1458(9)	0.1909(6)	0.0360(5)	0.052(5)	C(30)	0.6537(13)	0.1741(9)	0.3482(7)	0.041(6)
O(9)	1.2448(10)	0.0474(6)	0.0794(6)	0.071(5)	C(31)	0.5711(16)	0.1961(10)	0.4142(8)	0.049(7)
O(10)	0.7282(9)	0.1630(6)	0.1656(6)	0.054(5)	C(32)	0.5218(16)	0.2816(12)	0.4297(9)	0.065(8)
O(11)	1.3185(9)	0.2990(6)	0.1924(6)	0.054(5)	C(33)	0.5598(15)	0.3431(10)	0.3787(9)	0.055(7)
O(12)	0.634(3)	0.8522(13)	0.3490(13)	0.215(19)	C(34)	0.6481(14)	0.3177(9)	0.3153(8)	0.046(6)
O(13)	0.6398(23)	0.9165(8)	0.4424(7)	0.156(13)	C(35)	0.8561(20)	0.1268(12)	0.5613(9)	0.082(10)
O(14)	0.7041(18)	0.7697(8)	0.4392(7)	0.117(8)	C(36)	0.8646(16)	0.5213(8)	0.2108(8)	0.042(7)
O(15)	0.8302(23)	0.8493(13)	0.3709(14)	0.203(16)	C(37)	0.7782(19)	0.5643(11)	0.2679(9)	0.066(8)
O(16)	0.423(5)	0.607(4)	0.4104(22)	0.46(4)	C(38)	0.8026(22)	0.6364(14)	0.2860(11)	0.092(11)
N(1)	1.1180(11)	0.3267(7)	0.3199(6)	0.039(5)	C(39)	0.9175(23)	0.6665(11)	0.2492(11)	0.084(11)
N(2)	1.2607(10)	0.1606(7)	0.2912(7)	0.040(5)	C(40)	1.0042(18)	0.6196(10)	0.1916(10)	0.062(8)
N(3)	0.8348(11)	0.0681(7)	0.2718(6)	0.041(5)	C(41)	0.9755(16)	0.5500(9)	0.1716(8)	0.047(7)
N(4)	0.6931(11)	0.2341(7)	0.3008(6)	0.040(5)	C(42)	0.8619(14)	0.4193(9)	0.0373(8)	0.044(7)
C(1)	0.9613(13)	0.1859(9)	0.3375(8)	0.039(6)	C(43)	0.8137(16)	0.3557(10)	0.0170(9)	0.054(8)
C(2)	0.9380(13)	0.1051(9)	0.3621(8)	0.041(6)	C(44)	0.7208(18)	0.3819(13)	-0.0211(9)	0.065(9)
C(3)	0.9063(15)	0.0868(9)	0.4332(9)	0.047(7)	C(45)	0.6754(17)	0.4657(13)	-0.0412(9)	0.066(9)
C(4)	0.8928(16)	0.1446(12)	0.4810(9)	0.058(8)	C(46)	0.7284(18)	0.5266(12)	-0.0216(9)	0.068(8)
C(5)	0.9147(14)	0.2268(11)	0.4570(9)	0.050(7)	C(47)	0.8184(15)	0.5045(9)	0.0199(8)	0.050(7)
C(6)	0.9451(14)	0.2474(10)	0.3855(8)	0.045(7)	C(48)	1.2520(14)	0.2220(9)	-0.0112(8)	0.043(7)
C(7)	0.9762(14)	0.3325(9)	0.3582(8)	0.046(7)	C(49)	1.3812(18)	0.2066(12)	-0.0015(8)	0.066(9)
C(8)	1.1385(15)	0.4147(9)	0.2983(8)	0.045(7)	C(50)	1.4818(20)	0.2347(13)	-0.0488(10)	0.074(9)
C(9)	1.2743(14)	0.4233(9)	0.2568(8)	0.041(6)	C(51)	1.4547(20)	0.2794(12)	-0.1083(12)	0.078(10)
C(10)	1.3243(19)	0.4921(11)	0.2667(10)	0.069(9)	C(52)	1.3250(22)	0.2959(12)	-0.1182(10)	0.084(10)
C(11)	1.4480(19)	0.5075(12)	0.2270(11)	0.072(10)	C(53)	1.2264(18)	0.2651(10)	-0.0695(9)	0.063(8)
C(12)	1.5196(17)	0.4520(11)	0.1775(9)	0.056(8)	C(54)	1.1980(14)	-0.0266(9)	0.0848(10)	0.043(7)
C(13)	1.4859(15)	0.3822(10)	0.1644(9)	0.047(7)	C(55)	1.1513(17)	-0.0448(11)	0.0315(10)	0.067(9)
C(14)	1.3570(18)	0.3678(10)	0.2047(9)	0.053(8)	C(56)	1.1025(22)	-0.1177(14)	0.0356(15)	0.098(13)
C(15)	1.2118(16)	0.2828(9)	0.3612(8)	0.047(7)	C(57)	1.1061(21)	-0.1700(14)	0.0912(18)	0.092(12)
C(16)	1.2552(15)	0.1875(10)	0.3537(8)	0.043(7)	C(58)	1.1587(25)	-0.1571(13)	0.1449(13)	0.093(11)
C(17)	1.2944(17)	0.1330(12)	0.4053(10)	0.061(9)	C(59)	1.2094(18)	-0.0816(13)	0.1392(10)	0.071(9)

Figure 2. Molecular structure of $[\text{Fe}_2\text{bhpp}(\text{O}_2\text{P}(\text{OPh})_2)_2]\text{BPh}_4\cdot\text{CHCl}_3\cdot\text{CH}_3\text{OH}$, 3 with atomic designations in the backbone.

tammetry experiments were performed with a Metrohm instrument (Type 663 VA-Stand). The supporting electrolyte was 0.1 M tetra-*n*-butylammonium perchlorate in acetonitrile. Cyclic voltammograms were obtained by using a platinum disk working electrode, a carbon auxiliary electrode, and a saturated calomel reference electrode. Magnetic susceptibility data were obtained on polycrystalline samples over a

temperature range 4.2–290.0 K with a Faraday-type magnetometer which was calibrated with $\text{Co}[\text{Hg}(\text{SCN})_4]$. Pascal's^{32,33} constants were used to calculate the diamagnetic corrections. The theoretical expression was fitted to the data by applying least-squares refinements. Mössbauer spectra were measured at various temperatures against a $^{57}\text{Co}(\text{Rh})$ source moving in a mode of constant acceleration. Velocity calibration was carried out by the resonance lines of metallic iron, and isomer shifts were given relative to iron metal at room temperature.

X-ray Crystallography. Crystal data as well as details of data collection and refinement are summarized in Table 1. Blue crystals of 3 ($0.12 \times 0.15 \times 0.33$ mm) and 4 ($0.12 \times 0.15 \times 0.05$ mm) were mounted on a glass fiber and placed on a Syntex P2₁ (3) and a Siemens R3 (4) diffractometer ($\text{Mo K}\alpha$, $\lambda = 0.71073 \text{ \AA}$, graphite monochromator). Cell constants and orientation matrices were determined using least-squares refinements of the angular coordinates of 22 (3) and 18 (4) accurately centered reflections. Intensity data were collected by using the ω -scan (3) and the ω -2 θ -scan (4) techniques to maximum 2θ values of 48.0°. As a check of crystal and electronic stability, 2 representative reflections were measured every 98 data points. No significant trend in their intensities was observed during the course of data acquisition. Lorentz and polarization corrections were applied to the data, but no extinction and absorption corrections were carried out. Both structures were solved by using Patterson and Fourier methods (SHELXTL PLUS program package). Neutral-atom scattering factors were taken from ref 34. All non-H atoms were refined with anisotropic thermal parameters. Hydrogen atoms were included in calculated positions ($\text{C}-\text{H} = 0.96 \text{ \AA}$). U_{H} values were refined for both structures: for 3, $U_{\text{H}}(\text{CH}_2) = 0.115 \text{ \AA}^2$, $U_{\text{H}}(\text{CH}_{\text{arom}})$

(32) Carlin, R. L. In *Magnetochemistry*; Springer-Verlag: New York, 1986; p 3.

(33) O'Connor, C. J. *Prog. Inorg. Chem.* 1982, 29, 203–283.

(34) *International Tables for X-Ray Crystallography*; Kynoch Press: Birmingham, U.K., 1974; Vol. 4, pp 55, 99, and 149.

Table 4. Selected Bond Distances (\AA) for 3 and 4

	Compound 3			Compound 4			
	Fe(1)…P(1)	3.549(3)	Fe(2)…P(1)	3.282(4)	Fe(1)…P(1)	3.837(8)	
Fe(1)…P(2)	3.282(4)	Fe(2)…P(2)	3.207(5)	Fe(1)…P(2)	3.280(9)	Fe(2)…P(1)	3.237(9)
Fe(1)…O(1)	3.134(3)	Fe(1)…O(2)	2.103(9)	Fe(1)…O(1)	3.216(8)	Fe(2)…P(2)	3.274(9)
Fe(1)…O(7)	1.976(6)	Fe(1)…O(11)	1.889(10)	Fe(1)…O(6)	2.107(9)	Fe(1)…O(2)	2.017(9)
Fe(1)…N(1)	1.992(8)	Fe(1)…N(2)	2.125(9)	Fe(1)…N(1)	1.985(10)	Fe(1)…O(11)	1.854(11)
Fe(2)…O(1)	2.161(9)	Fe(2)…O(3)	2.044(9)	Fe(2)…O(1)	2.210(12)	Fe(1)…N(2)	2.137(12)
Fe(2)…O(6)	2.044(5)	Fe(2)…O(10)	1.855(6)	Fe(2)…O(7)	2.158(11)	Fe(2)…O(3)	1.980(9)
Fe(2)…N(3)	2.184(9)	Fe(2)…N(4)	2.164(10)	Fe(2)…N(3)	2.052(8)	Fe(2)…O(10)	1.852(12)
P(1)…O(2)	1.489(7)	P(1)…O(3)	1.486(7)	P(1)…O(2)	2.117(11)	Fe(2)…N(4)	2.130(10)
P(1)…O(4)	1.600(9)	P(1)…O(5)	1.571(9)	P(1)…O(4)	1.481(11)	P(1)…O(3)	1.472(11)
P(2)…O(6)	1.490(7)	P(2)…O(7)	1.484(6)	P(2)…O(6)	1.602(9)	P(1)…O(5)	1.573(9)
P(2)…O(8)	1.570(10)	P(2)…O(9)	1.567(9)	P(2)…O(8)	1.473(12)	P(2)…O(7)	1.472(10)
					1.557(10)	P(2)…O(9)	1.564(10)

Table 5. Selected Bond Angles (deg) for 3 and 4

	Compound 3			Compound 4			
	Fe(1)…O(1)…Fe(2)	124.0(3)		Fe(1)…O(1)…Fe(2)	128.2(4)		
O(1)…Fe(1)…O(2)	85.0(3)	O(1)…Fe(1)…O(7)	106.3(2)	O(1)…Fe(1)…O(2)	87.8(4)	O(1)…Fe(1)…O(6)	88.9(4)
O(1)…Fe(1)…O(11)	96.6(3)	O(1)…Fe(1)…N(1)	81.8(3)	O(1)…Fe(1)…O(11)	176.2(4)	O(1)…Fe(1)…N(1)	89.1(4)
O(1)…Fe(1)…N(2)	154.5(4)	O(2)…Fe(1)…O(7)	87.4(3)	O(1)…Fe(1)…N(2)	87.7(4)	O(2)…Fe(1)…O(6)	96.4(4)
O(2)…Fe(1)…O(11)	178.2(3)	O(2)…Fe(1)…N(1)	89.7(3)	O(2)…Fe(1)…O(11)	91.7(4)	O(2)…Fe(1)…N(1)	92.9(4)
O(2)…Fe(1)…N(2)	81.7(4)	O(7)…Fe(1)…O(11)	91.4(4)	O(2)…Fe(1)…N(2)	170.8(4)	O(6)…Fe(1)…O(11)	95.0(4)
O(7)…Fe(1)…N(1)	171.2(3)	O(7)…Fe(1)…N(2)	94.8(3)	O(6)…Fe(1)…N(1)	170.4(4)	O(6)…Fe(1)…N(2)	91.5(4)
O(11)…Fe(1)…N(1)	91.3(4)	O(11)…Fe(1)…N(2)	97.1(4)	O(11)…Fe(1)…N(1)	87.2(5)	O(11)…Fe(1)…N(2)	92.3(5)
N(1)…Fe(1)…N(2)	76.6(4)	O(1)…Fe(2)…O(3)	85.3(3)	N(1)…Fe(1)…N(2)	79.0(4)	O(1)…Fe(2)…O(3)	88.3(4)
O(1)…Fe(2)…O(6)	92.3(2)	O(1)…Fe(2)…O(10)	170.2(3)	O(1)…Fe(2)…O(7)	87.3(4)	O(1)…Fe(2)…O(10)	176.6(4)
O(1)…Fe(2)…N(3)	81.2(3)	O(1)…Fe(2)…N(4)	87.1(3)	O(1)…Fe(2)…N(3)	89.4(4)	O(1)…Fe(2)…N(4)	86.6(4)
O(3)…Fe(2)…O(6)	96.3(3)	O(3)…Fe(2)…O(10)	93.4(3)	O(3)…Fe(2)…O(7)	96.0(3)	O(3)…Fe(2)…O(10)	95.1(4)
O(3)…Fe(2)…N(4)	170.9(3)	O(3)…Fe(2)…N(3)	95.4(4)	O(3)…Fe(2)…N(3)	172.0(4)	O(3)…Fe(2)…N(4)	92.4(4)
O(6)…Fe(2)…O(10)	97.6(3)	O(6)…Fe(2)…N(3)	166.1(4)	O(7)…Fe(2)…O(10)	92.2(4)	O(7)…Fe(2)…N(3)	91.6(4)
O(6)…Fe(2)…N(4)	89.2(3)	O(10)…Fe(2)…N(3)	89.2(3)	O(7)…Fe(2)…N(4)	169.5(4)	O(10)…Fe(2)…N(3)	87.3(5)
O(10)…Fe(2)…N(4)	93.1(3)	N93)…Fe(2)…N(4)	78.3(4)	O(10)…Fe(2)…N(4)	93.5(4)	N(3)…Fe(2)…N(4)	79.8(4)
O(2)…P(1)…O(3)	118.6(5)	O(2)…P(1)…O(4)	104.0(4)	O(2)…P(1)…O(3)	119.5(6)	O(2)…P(1)…O(4)	110.5(6)
O(2)…P(1)…O(5)	112.2(4)	O(3)…P(1)…O(4)	111.0(4)	O(2)…P(1)…O(5)	104.2(5)	O(3)…P(1)…O(4)	105.5(6)
O(3)…P(1)…O(5)	105.1(4)	O(4)…P(1)…O(5)	105.3(5)	O(3)…P(1)…O(5)	110.2(6)	O(4)…P(1)…O(5)	106.4(5)
O(6)…P(2)…O(7)	115.9(4)	O(6)…P(2)…O(8)	104.5(5)	O(6)…P(2)…O(7)	119.0(6)	O(6)…P(2)…O(8)	111.5(6)
O(6)…P(2)…O(9)	113.0(4)	O(7)…P(2)…O(8)	112.6(4)	O(6)…P(2)…O(9)	106.4(6)	O(7)…P(2)…O(8)	105.3(6)
O(7)…P(2)…O(9)	104.4(5)	O(8)…P(2)…O(9)	106.2(5)	O(7)…P(2)…O(9)	109.2(6)	O(8)…P(2)…O(9)	104.5(6)

= 0.052 \AA^2 ; for 4, $U_{\text{H}}(\text{CH}_3) = 0.101 \text{\AA}^2$, $U_{\text{H}}(\text{CH}_2) = 0.034 \text{\AA}^2$, $U_{\text{H}}(\text{CH}_{\text{arom}}) = 0.070 \text{\AA}^2$. Hydrogen atom positions were not refined independently in either structure. The coordinates of the atoms in the unit cells and the equivalent thermal parameters are given for 3 in Table 2 and for 4 in Table 3.

Results and Discussion

Description of the X-ray Structures. $[\text{Fe}_2\text{bhpp}(\text{O}_2\text{P}(\text{OPh})_2)_2\text{BPh}_4\cdot\text{CHCl}_3\cdot\text{H}_2\text{O}$, 3. Compound 3 crystallizes in the triclinic space group $\bar{P}\bar{1}$. The structure of the cation of 3 is shown in Figure 2, and selected bond lengths and angles are given in Tables 4 and 5. The structure of 3 reveals that both Fe(III) ions are coordinated by the heptadentate ligand bhpp³⁻; each metal ion is bonded to one pyridine moiety, one tertiary nitrogen atom, the phenolate oxygen atom, and the bridging alkoxo oxygen atom. The distorted octahedral environment of each iron center is completed by coordination of two diphenyl phosphato ligand molecules. Though the metal centers in 3 are coordinated by a N_2O_4 -donor set, the environments of both iron ions are not equivalent. This asymmetry is the result of significant differences found for the Fe–O(1) bond lengths of both iron centers. The length of the Fe(1)–O(1) bond is 1.976(6) \AA , while that for Fe(2)–O(1) is significantly larger (2.044(5) \AA). Other Fe–O distances in $\text{Fe}_2(\mu\text{-OR})$ units for comparison include $[\text{Fe}_4\text{O}_2(\text{tbpo})_2(\text{OBz})_2]^{4+}$ (1.995 and 2.018 \AA),³⁵ $[\text{Fe}_4\text{O}_2(\text{pta})_2(\text{CO}_3)_2]^{4-}$ (2.040 and 2.066 \AA),³⁶ $[\text{Fe}_2(\text{pta})(\text{OBz})(\text{H}_2\text{O})_2]$ (1.981 and 2.006

\AA),³⁷ and $[\text{Fe}_2\text{Cl}_2\{\text{O}_2\text{P}(\text{OPh})_2\}(\text{tbpo})(\text{MeOH})]^{2+}$ (2.011 and 2.066 \AA).¹⁸ The larger difference between the Fe–O(alkoxo) bond lengths in 3 may be ascribed to a structural trans effect of the short Fe(2)–O(10)(phenolate) bond (1.855(6) \AA) which is trans to O(1), whereas at Fe(1) the corresponding oxygen atom O(11) is cis to the bridging O(1). Furthermore, the shorter Fe–O_{phosphate} bonds are exhibited by the oxygen atoms that are trans to the tertiary amino nitrogen atoms N(1) and N(3) (Fe(1)–O(7) = 1.992(8) \AA , Fe(2)–O(6) = 1.992(8) \AA —an effect which has also been observed for the carboxylate complexes $[\text{Fe}^{\text{II}}\text{Fe}^{\text{III}}\text{bpmp}(\text{OPr})_2]^{2+}$ and $[\text{Zn}^{\text{II}}\text{Fe}^{\text{III}}\text{bpmp}(\text{OAc})_2]^{2+}$.³¹ The Fe…Fe distance of 3.549 \AA compares favorably with the metal–metal separations found in $[\text{Fe}_4\text{O}_2(\text{tbpo})_2(\text{OBz})_2]^{4+}$ and $[\text{Fe}_4(\text{Et-tbpo})_2(\text{OAc})_2]^{4+}$ (3.608 and 3.488 \AA across the alkoxo bridges, respectively), though the bite distance of the phosphate is larger.³⁵

$[\text{Fe}_2\text{bhpp}(\text{O}_2\text{P}(\text{OPh})_2)_2]\text{ClO}_4\cdot\text{H}_2\text{O}$, 4. Complex 4 crystallizes in the triclinic space group $\bar{P}\bar{1}$. Figure 3 shows the structure of the cation of 4. Tables 4 and 5 contain selected bond lengths and angles, respectively. The molecule contains a μ -phenoxo-bridged $\text{Fe}^{\text{II}}\text{Fe}^{\text{III}}$ unit in which the metal centers are additionally linked by two μ -diphenyl phosphato bridges. The pendant pyridine and phenolate moieties as well as the tertiary nitrogen donors of the ligand bhpp³⁻ complete an octahedral environment of both metal centers. The Fe…Fe distance of 3.837 \AA in 4 is significantly larger than the metal–metal separation in 3 (3.549 \AA) or in $[\text{Fe}^{\text{II}}\text{Fe}^{\text{III}}\text{bpmp}(\text{O}_2\text{P}(\text{OPh})_2)_2](\text{ClO}_4)_2\text{CH}_3\text{OH}\cdot\text{H}_2\text{O}$ (3.694 \AA), which contains a (μ -phenoxo)bis(μ -diphenyl phosphato)diiron(II,III) core.¹² The Fe(1)–O(1)–Fe(2) angle is 128.3(4) $^\circ$, and the phenyl

(35) Chen, Q.; Lynch, J. B.; Gomez-Romero, P.; Ben-Hussein, A.; Jameson, G. B.; O'Connor, C. J.; Que, L., Jr. *Inorg. Chem.* 1988, 27, 2673–2681.
 (36) Jameson, D. L.; Xie, C.-L.; Hendrickson, D. N.; Potenza, J. A.; Schugar, H. J. *J. Am. Chem. Soc.* 1987, 109, 740–746.

(37) Kawata, S.; Nakamura, M.; Yamashita, Y.; Asai, K.; Kikuchi, K.; Ikemoto, I.; Katada, M.; Samo, H. *Chem. Lett.* 1992, 135–138.

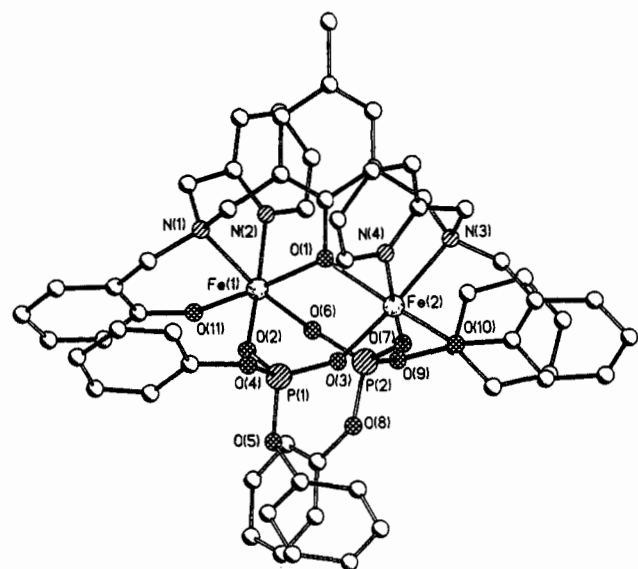


Figure 3. Molecular structure of $[\text{Fe}_2\text{bhpmp}(\text{O}_2\text{P}(\text{OPh})_2)_2]\text{ClO}_4 \cdot \text{H}_2\text{O}$, 4, with atomic designations in the backbone.

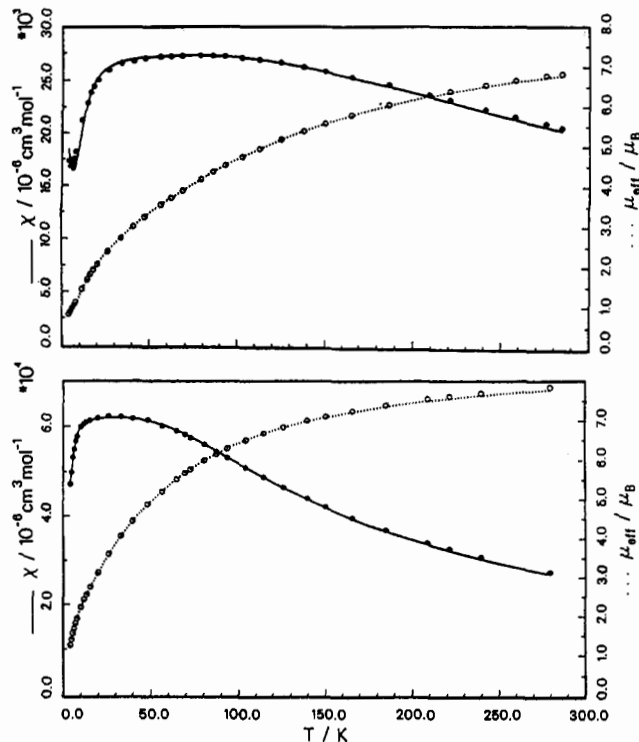


Figure 4. Temperature dependence of the corrected molar magnetic susceptibility χ_M and the experimental magnetic moment per dimer of 3 (top) and 4 (bottom).

ring of the bhpmp³⁻ ligand is twisted relative to the Fe(1)–O(1)–Fe(2) plane (55.2°). An analogous twist of the bridging phenolato ring from the Fe–O–Fe plane has also been observed in the carboxylato-bridged complex $[\text{Fe}^{\text{II}}\text{Fe}^{\text{III}}\text{bpmp}(\text{OPr})_2](\text{BPh}_4)_2\text{CH}_3\text{COCH}_3 \cdot 0.5\text{CH}_3\text{CN}$ ³¹ as well as in the diphenyl phosphato-bridged complex $[\text{Fe}^{\text{II}}\text{Fe}^{\text{III}}\text{bpmp}(\text{O}_2\text{P}(\text{OPh})_2)_2](\text{ClO}_4)_2\text{CH}_3\text{OH} \cdot \text{H}_2\text{O}$,¹² in which dihedral angles of 51.3 and 54.6° were observed, respectively. The lengths of the Fe(1)–O(1) and the Fe(2)–O(1) bonds (2.107(9) and 2.158(11) Å) are significantly larger than the Fe(III)–O(phenolate) bonds in $[\text{Fe}^{\text{II}}\text{Fe}^{\text{III}}\text{bpmp}(\text{OPr})_2]^{2+}$ (1.943(2) Å),³¹ $[\text{Fe}^{\text{II}}\text{Fe}^{\text{III}}\text{bpmp}(\text{O}_2\text{P}(\text{OPh})_2)_2]^{2+}$ (1.955(3) Å),¹² and $(\text{Me}_4\text{N})[\text{Fe}^{\text{III}}\text{xta}(\text{OAc})_2] \cdot \text{H}_2\text{O}$ (1.997(2) and 2.019(2) Å).³⁸

(38) Murch, B. P.; Bradley, F. C.; Que, L., Jr. *J. Am. Chem. Soc.* 1986, 108, 5027–5028.

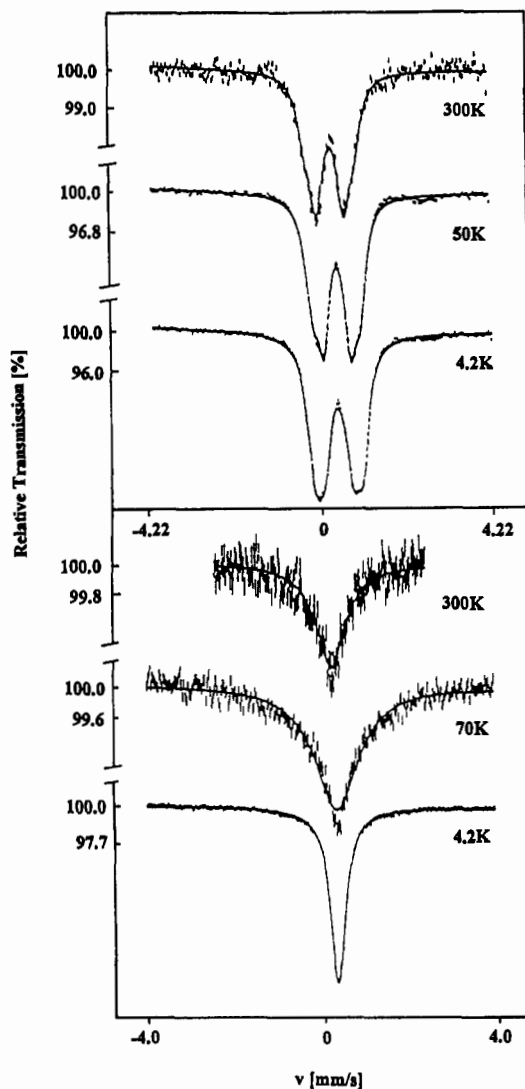


Figure 5. ^{57}Fe Mössbauer spectra of polycrystalline samples of 3 (top) and 4 (bottom) at different temperatures.

These unusually long Fe–O bonds in 4 can be ascribed to the structural trans effect of the short Fe(1)–O(11) and Fe(2)–O(10) bonds (1.854(11) and 1.852(12) Å). In the cation of 4, each of the metal centers has a tertiary amino nitrogen atom and the pyridyl group trans to oxygen atoms of the diphenyl phosphato bridges. The shorter Fe(1)–O(6) (1.985(10) Å) and Fe(2)–O(3) (1.980(9) Å) bonds are exhibited by the diphenyl phosphato oxygen atoms that are trans to the tertiary amino nitrogen atoms (N(1) and N(3)). The bond lengths Fe(1)–N(1) (2.210(12) Å) and Fe(2)–N(3) (2.177(11) Å) are longer than the Fe–N_{pyridine} bonds (Fe(1)–N(2) = 2.137(12) Å, Fe(2)–N(4) = 2.130(10) Å). Similar differences concerning the Fe–N bonds were observed in $[\text{Fe}^{\text{II}}\text{Fe}^{\text{III}}\text{bpmp}(\text{OPr})_2]^{2+}$ and have been ascribed to constraints associated with the short, one carbon “arm lengths” from the phenolato ring and the pyridyl ring to the tertiary amino nitrogen atom.³¹

Magnetic Susceptibility Measurements. Solid-state magnetic susceptibility measurements on crystalline samples of 3 and 4 were made by using the Faraday method in the range between 4.2 and 290 K and indicate the presence of antiferromagnetic coupling with room-temperature μ_{eff} values of 6.838 μ_B (284.5 K) and 7.838 μ_B (279.5 K). The magnetic moments of both complexes decrease at 4.2 K to 0.763 μ_B (3) and 1.244 μ_B (4) (Figure 4). The values could be fitted on the basis of an isotropic Heisenberg model, $H' = -2JS_1S_2$ ($S_1 = S_2 = 5/2$) and $g = 2.0$ (fixed).³³ The coupling constant found for 3 ($J = -12.5(3)$ cm⁻¹) represents the typical range for μ -alkoxo- or μ -hydroxo-bridged

Table 6. Mössbauer Parameters

3						
T, K	δ_1 , mm/s	ΔE_{Q1} , mm/s	Γ_1 , mm/s	δ_2 , mm/s	ΔE_{Q2} , mm/s	Γ_2 , mm/s
300	0.40	0.66	0.43	0.40	1.22	0.40
50	0.52	0.65	0.36	0.51	1.17	0.38
4.2	0.51	0.71	0.43	0.52	1.21	0.39
4						
T, K	δ , mm/s	Γ , mm/s	T, K	δ , mm/s	Γ , mm/s	
300	0.36	0.82	4.2	0.44	0.42	
70	0.48	1.24				

The figure contains two cyclic voltammograms. The top one, for complex 3, shows two reversible one-electron waves at approximately +60 mV and -800 mV versus SCE. The bottom one, for complex 4, shows a reversible electron transfer at $E_1 = -200$ mV.

Figure 6. Cyclovoltammograms of 3 (top) and 4 (bottom).

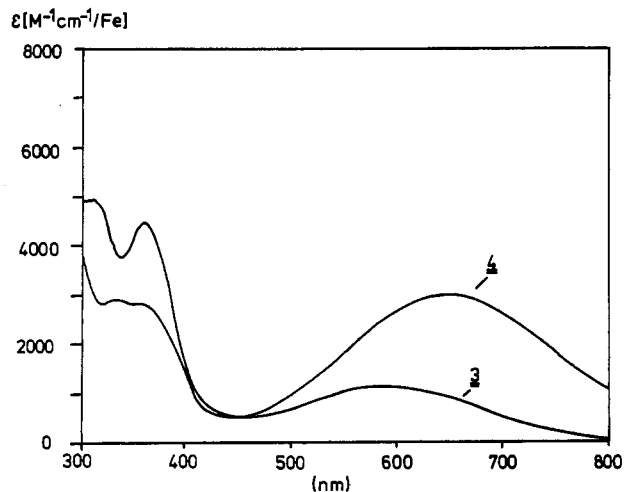


Figure 7. Electron absorption spectra of 3 and 4 in the visible region.

dinuclear Fe(III) systems, while that for 4 ($J = -5.6(1) \text{ cm}^{-1}$) is smaller than in the μ -phenoxy-bridged complexes $[\text{Fe}_2\text{bpmp}(\text{C}_6\text{H}_5\text{COO})_2](\text{ClO}_4)_3\text{CH}_3\text{CN}\cdot\text{H}_2\text{O}$ ($J = -12 \text{ cm}^{-1}$)³⁹ $[\text{Fe}_2(\text{L}-\text{bzim})(\text{CH}_3\text{COO})_2](\text{ClO}_4)_3\cdot 3.5\text{H}_2\text{O}$ ($J = -8.8 \text{ cm}^{-1}$).³⁹ This

weaker antiferromagnetic behavior reflects the larger Fe–O(bridge) bond lengths in 4, due to the trans effect of the phenolate oxygen atoms O(10) and O(11). The magnetic coupling constants in 3 and 4 are smaller than the values to be expected for μ -hydroxo- or μ -oxo-bridged systems. As discussed above, these bridge types are proposed by Que et al.⁸ and Averill et al.⁴ for the mammalian purple phosphatases. In this sense, the present models are not consistent with the picture of an oxo-bridged unit in the enzymes, however, rather consistent with an alkoxo (or hydroxo) bridge.

Mössbauer Spectra. The ^{57}Fe Mössbauer spectra of 3 and 4 are given in Figure 5, and their parameters are listed in Table 6. The spectra of both complexes confirm the existence of octahedral high-spin Fe(III) ions. The Mössbauer spectrum of 3 as a crystalline solid at 4.2 K exhibits two distinct quadrupole doublets of equal intensity having δ values of 0.51 and 0.52 mm/s and ΔE_Q values of 0.71 and 1.21 mm/s. The quadrupole splittings reflect different electric field gradients at the nucleus, suggesting a nonequivalent environment of both iron ions, which corroborates the crystallographic results for 3. Interestingly, the Mössbauer spectra of 4 show only one line in the range from 4.2 to 300 K indicating considerably smaller field gradients than in 3. At 4.2 K the line width is comparable to that of the spectrum of 3. The two iron sites are not distinguishable in the Mössbauer spectrum; thus, the charge distribution appears to be nearly spheric for both sites. The causes of this different balance within the electronic distribution of 3 and 4 in spite of rather similar geometrical and symmetry properties of the first-shell iron coordinations are not yet completely understood.

Electrochemistry. Electrochemical investigations on 3 and 4 were carried out in order to examine the redox properties of these complexes. The cyclic voltammograms of 3 and 4 are shown in Figure 6. In acetonitrile with $[\text{TBA}] \text{ClO}_4$ as the supporting electrolyte, 3 exhibits two irreversible one-electron waves at +60 and -800 mV versus SCE, which are assigned to the $\text{Fe}^{\text{III}}/\text{Fe}^{\text{II}}$ and $\text{Fe}^{\text{II}}/\text{Fe}^{\text{III}}$ couples transitions, respectively. The irreversible oxidation wave at +900 mV is due to the oxidation of the BPh_4^- anion. In case of 4 a reversible electron transfer is observed at $E_1 = -200$ mV, which corresponds to the $\text{Fe}^{\text{III}}/\text{Fe}^{\text{II}}$ couple. Further reduction gives rise to an irreversible reduction wave at -840 mV.

Electronic Absorption Properties. The visible absorption spectra in methylene chloride for the complexes 3 and 4 are displayed in Figure 7. 3 exhibits a UV-vis spectrum with features at 315 ($\epsilon \approx 4910 \text{ M}^{-1} \text{ cm}^{-1}/\text{Fe}$), 361 ($\epsilon \approx 4625 \text{ M}^{-1} \text{ cm}^{-1}/\text{Fe}$), and 586.5 nm ($\epsilon \approx 1150 \text{ M}^{-1} \text{ cm}^{-1}/\text{Fe}$). The absorption spectrum of 4 consists of three absorption maxima centered at 340 ($\epsilon \approx 2770 \text{ M}^{-1} \text{ cm}^{-1}/\text{Fe}$), 361.5 ($\epsilon \approx 2750 \text{ M}^{-1} \text{ cm}^{-1}/\text{Fe}$), and 649 nm ($\epsilon \approx 2960 \text{ M}^{-1} \text{ cm}^{-1}/\text{Fe}$). The main features in the electronic spectra of both complexes are the relatively intense charge-transfer (CT) bands that give rise to the bluish colors and which are assigned to a transition from the p_z orbital on the phenolate oxygen atom to d_{z^2} orbitals of the ferric ion. According to previous studies, the lower energy bands in the spectra of 3 and 4 are associated with the phenolate to Fe(III) CT transition, while the higher energy bands may be assigned as a $p_z \rightarrow d_{z^2}$ type.

Intensities and positions of phenolate–Fe(III) charge-transfer transitions depend on several factors, but in general synthetic complexes have extinction coefficients of 1000 – $2000 \text{ M}^{-1} \text{ cm}^{-1}/\text{Fe(III)}\text{-phenolate bond}$. Generally, it is rather difficult to set up clear correlations between the extremely variable extinction coefficients in Fe(III)–phenolate units and structural and electrochemical parameters. A priori, the presence of the bridging phenolate group in 4 should give rise to higher energy LMCT bands as compared to 3. Certainly, there is no simple correlation to be expected between the number of phenoxide groups and gross band intensities. A larger absorption coefficient has been observed in $[\text{Fe}_2(\text{hdp})_2\text{O}(\text{OBz})]\text{BPh}_4$,⁴⁰ which exhibits the ab-

(39) Suzuki, M.; Oshio, H.; Uehara, A.; Endo, M. Y.; Kida, S.; Saito, K. *Bull. Chem. Soc. Jpn.* 1988, 61, 3907–3913.

(40) Yan, S.; Que, L., Jr. *J. Am. Chem. Soc.* 1988, 110, 5222–5224.

sorption maximum of the CT transition at 522 nm ($\epsilon \approx 3300 \text{ M}^{-1} \text{ cm}^{-1}$).

Acknowledgment. We thank Burkhard Eulering and Michael Schmidt for valuable discussions, and we thank Bettina Bremer for her excellent technical assistance. Thanks are also due to one of the reviewers for constructive comments on the UV-vis spectra,

to the Deutsche Forschungsgemeinschaft, and to the Fonds der Chemischen Industrie for financial support.

Supplementary Material Available: Crystallographic data for the compounds in Table 1, including tables of H coordinates, complete bond lengths and angles, and anisotropic thermal parameters (14 pages). Ordering information is given on any current masthead page.